Luchian Andreea (Orcid ID: 0000-0001-7959-6190)

Manuscript title: Combined Colour Deconvolution and Artificial Intelligence approach for region-selective immunohistochemical labelling quantification. The example of alpha Smooth Muscle Actin in mouse kidney.

Short running title: Colour Deconvolution & AI for IHC Label Quantification

Full information on authors:

Andreea Luchian, Email: A.Luchian@liverpool.ac.uk, Phone number: +447495658616, ORCID ID: 0000-0001-7959-6190

Lorenzo Ressel, Email: ressel@liverpool.ac.uk, Phone number: +447713250422, ORCID ID: 0000-0002-6614-1223

Affiliation: Department of Veterinary Anatomy Physiology and Pathology, Institute of infection veterinary and ecological science, University of Liverpool, UK

Full address: Department of Veterinary Anatomy Physiology and Pathology, Institute of Infection, Veterinary and Ecological Sciences, University of Liverpool, Leahurst Campus, Chester High Road, Neston, CH64 7TE

Disclosures: We have no conflicts of interest to disclose

Keywords: “colour-deconvolution”, “artificial-intelligence”, “immunohistochemistry”, “co-localisation”, “alpha Smooth Muscle Actin”, “glomeruli”, “mouse”

This article has been accepted for publication and undergone full peer review but has not been through the copyediting, typesetting, pagination and proofreading process which may lead to differences between this version and the Version of Record. Please cite this article as doi: 10.1002/jbio.202300244

ABSTRACT

Immunohistochemical (IHC) localisation of protein expression is a widely used tool in pathology. This is semi-quantitative and exhibits substantial intra-and inter-observer variability. Digital approaches based on stain quantification applied to IHC are precise but still operator-dependent and time-consuming when regions of interest (ROIs) must be defined to quantify protein expression in a specific tissue area. This study aimed at developing an IHC quantification workflow that benefits from colour deconvolution for stain quantification and artificial intelligence for automatic ROI definition. The method was tested on 10 Whole Slide Images (WSI) of Alpha-Smooth Muscle Actin (aSMA) stained mouse kidney sections. The task was to identify aSMA-positive areas within the glomeruli automatically. Total aSMA detection was performed using two channels (DAB, haematoxylin) colour deconvolution. Glomeruli segmentation within the same IHC WSI was performed by training a convolutional neural network with annotated examples of glomeruli. For both aSMA and glomeruli, binary masks were created. Co-localisation was performed by overlaying the masks and assigning red/green colours, with yellow indicative of a co-localised signal. The workflow described and exemplified using the case of aSMA expression in glomeruli can be applied to quantify the expression of IHC markers within different structures of immunohistochemically stained slides. The technique is objective, has a fully automated threshold approach (colour deconvolution phase) and uses AI to eliminate operator-dependent steps.

Introduction

The expression and localisation of proteins are key to the understanding of physiological and pathological mechanisms. A well-established method for identifying specific antigens in tissue sections is immunohistochemistry (IHC) (1–3). After labelling with specific antibodies and revelation systems, proteins of interest are commonly visualised in brightfield light using chromogen 3,3′-Diaminobenzidine (DAB). In a standardised experiment, despite the lack of true quantitative power, a stronger DAB intensity corresponds to a higher protein expression in the tissue despite the absence of a stochiometric connection between the intensity of the chromogen and the amount of antigen present (4). Semiquantitative IHC intensity scoring is frequently approached in diagnostics and research environments to assess the amount of protein expressed and typically uses a four-point scale (0, 1, 2, 3 or absent, mild, moderate, severe)(5–7). This semi-quantitative method, however, exhibits substantial intra-and inter-observer variability and can be highly subjective and inaccurate (8). The use of digital image analysis, which is valuable for automating workflows, represents a solution to improve repeatability and consistency (9). With the advent of whole slide images (WSI) and the increase in computational power available to investigators, digital image analysis on a WSI is possible and within reach (10). However, even when digital image analysis based on colour identification is applied to immunohistochemically stained slides, two main challenges remain: Firstly, the presence of false positive areas arising from possible background staining or similarly coloured structures (e.g., melanin, hemosiderin, bile pigments) necessitates manual removal to avoid overestimation of protein expression (11,12). Secondly, in scenarios where the protein expression of interest is confined to a specific tissue compartment or region of interest (ROI), analysing the entire tissue as a whole, introduces bias, particularly when other regions express the protein at baseline levels under normal conditions. Addressing this concern requires the manual creation of ROIs to compensate for the potential bias, which is a time-consuming step reliant on human input.

In the context of a healthy kidney, the immunohistochemical expression of Alpha-smooth muscle actin (aSMA) is confined primarily to vascular smooth muscle cells, with a secondary presence in the kidney capsule. Nevertheless, under specific pathological conditions, the expression of aSMA may extend to encompass certain glomerular mesangial cells and interstitial myofibroblasts, as evidenced in relevant literature (13,14). In an experimental scenario focused on the quantification of aSMA within glomeruli as a consequence of tissue damage, the utilisation of automated techniques for quantifying the DAB colouration

throughout the entire Whole Slide Image (WSI) could introduce a significant degree of "background noise" data. This occurs unless we manually select ROIs or exclude non-ROI areas, thereby resulting in a labour-intensive process.

In recent years, Artificial intelligence and, in particular, Deep Learning (DL) using Convolutional Neural Networks (CNN) have revolutionised the strategy to automatically classify or segment specific areas of images based on their patterns in a similar way to a human (15). While this approach has primarily been applied to haematoxylin and eosin (HE) stained sections thus far (16), the objective of this study is to propose a generic and open workflow where immunomarkers need to be automatically quantified within a specific tissue compartment on a single IHC-stained slide. To demonstrate this concept as a proof of principle, we combined colour deconvolution to obtain a global quantification of the immunohistochemical staining (aSMA) and deep learning to detect and segment the tissue compartment (Glomeruli) in a mouse kidney. The resulting image overlays were merged as a final step, and co-localisation was detected based on the coloured pixels that corresponded both to glomeruli and SMA stain, leading to a precise quantification of aSMA expression within the glomerular area only.

Methods

For immunohistochemistry, 4-µ-thick sections were obtained from formalin-fixed paraffin-embedded tissue samples (FFPEs) of mouse kidneys originating from previous experiments of chronic IRI mouse models of kidney injury (17). Antigen retrieval was performed by calibrated water bath capable of maintaining the epitope retrieval solution (10 mM sodium citrate buffer pH 6.0) at 97 °C for 30 min (Agilent Technologies Ltd., Stockport, UK). The sections were allowed to cool down to room temperature for 20 min. Endogenous peroxidase was blocked using 100 µL Dako REALTM peroxidase blocking solution for 10 min (Agilent Technologies Ltd., Stockport, UK). Rabbit polyclonal to alpha smooth muscle Actin antibody (ab5694, Abcam, Cambridge, UK) diluted 1:500 was added and incubated overnight at +4°C. This was followed by a 30-minute incubation at room temperature with the secondary antibody and polymer peroxidase-based detection system (Anti Rabbit Envision+, Agilent Technologies Ltd). The reaction was visualised with diaminobenzidine (DAB- Agilent Technologies Ltd) at room temperature after 5' application and subsequent wash. Consecutive sections incubated with monoclonal rabbit unrelated monoclonal antibody served as negative control. The positive reaction was represented by a distinct brown cytoplasmic reaction. Slides were mounted with

a coverslip using a xylene-based mounting media. aSMA-stained slides were digitally scanned using an Aperio CS2 slide scanner (Leica Biosystems, Nussloch, Germany), with Plan Apo 20X objective lens setup, and visualised using ImageScope™ software (Leica Biosystems, Nussloch, Germany). Phase 1 consisted of aSMA staining detection using colour deconvolution by specifying a stain matrix for both the Haematoxylin (H) and Diaminobenzidine (DAB) stainings (18,19). The stain matrix used in this study represented the colour of each stain through optical density, expressed as a unit vector indicating the relative attenuation of red, green, and blue channels. For channel one (Haematoxylin), the optical density values are as follows: red = 0.650, green = 0.704, and blue = 0.286. Similarly, for channel two (Diaminobenzidine), the optical density values are red = 0.268, green = 0.570, and blue = 0. 776. After the separation of staining, masks were created for the DAB channel only, where the stain of interest is represented by white pixels (R255, G255, B255) over a black background (R0, G0, B0). Phase 2 consisted of glomeruli segmentation on the same IHC-stained WSI using deep learning, implementing a CNN with UNET architecture (20). 10 WSIs were used in this experiment. To train the network, a total number of 1131 annotation examples of 3 classes representing glomeruli, kidney tissue (any morphological structure of the kidney except glomeruli) and background (area of the slide characterised by the homogeneous white area without the presence of any histological structure) were created as an output for the DL algorithm. Examples of glomeruli included all ranges of aSMA-stained intensity. The employed CNN model was trained at a learning magnification of 20X for 2550 epochs and a learning rate of 5.00E-06. The computer system used was equipped with 4x Nvidia® Quadro® RTX8000 GPUs (Nvidia, Santa Clara, California) using dedicated software MIMPro (Medical Image Manager Pro with Deep Learning Add On; HeteroGenius®) based on TensorFlow library, which was used for both Phase 1 and 2. To evaluate the CNN's performance, we constructed a multiclass confusion matrix. From this matrix, we extracted several key metrics for each class, including precision (the fraction of predictions that were true positives), recall (sensitivity), specificity, and F1 score (the harmonic mean of precision and recall). These metrics allowed us to calculate the overall model accuracy, mean precision, recall and F1 (21,22).

After the learning process finished, a black-and-white overlay image (mask) was created where each pixel classified as glomeruli were assigned as white (R255, G255, B255), and each pixel classified as either kidney or background was assigned as black (R0, G0, B0). The overlays created using DL and colour deconvolution were size-matched, as performed from the WSI.

Using Fiji software (23), a pure RGB colour was assigned: red (R255, G0, B0) for the glomeruli in the CNN image; Green (R0, G255, B0) for the aSMA immunostaining in the colour deconvolution image. The two images were then merged into one image, where the co-localisation of each pixel was expressed as yellow pixels (R255, G255, B0). A colour threshold was then applied for the hue range of yellow and measured. Consequently, the colour threshold was set to pick up the whole range of coloured pixels, and measurement was performed. Then, a series of different quantifications were performed for the yellow pixels area (23). Total aSMA stain within glomeruli was normalised over the glomerular total area, the total Kidney aSMA stain and the total kidney surface.

Results

The immunohistochemical stain of aSMA was successful (Fig. 1A) and allowed a precise colour deconvolution for the aSMA stain (Fig. 1B). The CNN training process yielded favourable results, demonstrating an overall model accuracy of 0.96. Furthermore, the mean precision, a measure of the proportion of correctly predicted positive samples, was found to be 0.97. The mean recall or sensitivity, which quantifies the proportion of actual positive samples correctly identified by the model, also achieved a value of 0.97. Lastly, the mean F1 score, a harmonic mean of precision and recall, reached a value of 0.96, indicating a balanced performance between precision and recall. Consequently, the mask obtained overlapped correctly with the glomeruli area visible in the IHC stained slide (Fig 1 C). The merged coloured image efficiently shows the aSMA expression within the glomeruli as a yellow signal representing co-localised pixels for aSMA stain and glomerular area (Fig 1 D). Crucially, the CNN identification of the glomerular area was irrespective of aSMA intensity expression, as clearly shown by a comparison of an intensely aSMA-stained glomerulus (Fig. A, B, C arrow) to a very poorly stained one (Fig. A, B, C arrowhead). Identification of the glomerular area and aSMA stain allowed different quantifications; a non-comprehensive list of possible measurements is summarised in Table 1.

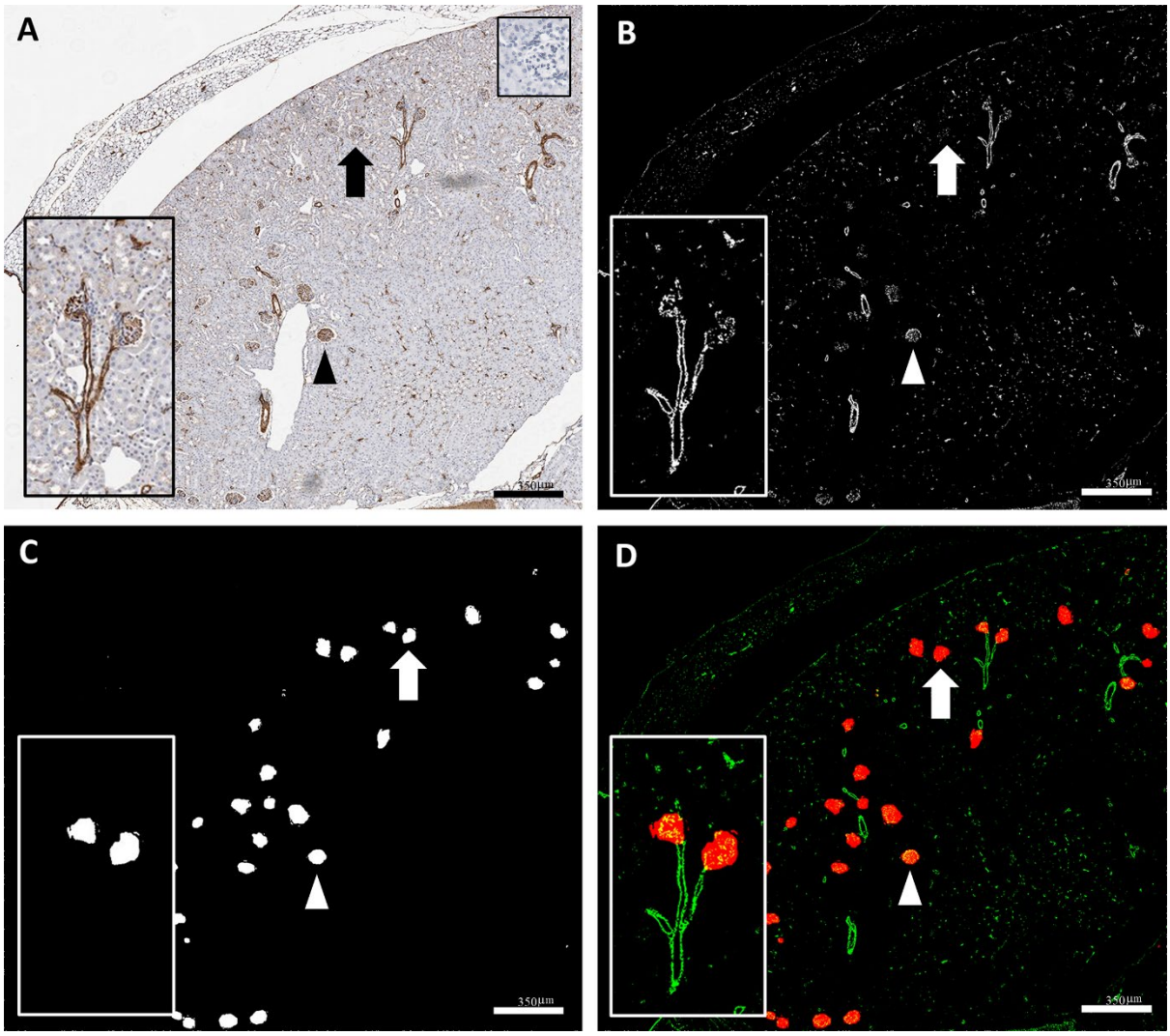

Figure 1: Immunohistochemical localisation of aSMA in the mouse kidney glomeruli. A: aSMA-positive areas were detected in the blood vessels, glomeruli and interstitium on IHC stained slide; Arrow: poorly aSMA-stained glomerulus; Arrowhead: intensely aSMA-stained glomerulus. Lower left Insert: higher magnification of a glomerulus and associated blood vessels. Higher right Insert: Glomerulus and tubules negative control B: aSMA staining detection using colour deconvolution; Arrow: Barely evident aSMA stain on a glomerulus; Arrowhead: intense aSMA stain on a glomerulus. Insert shows aSMA detection both in vessels and glomerular structures. C: Glomeruli segmentation using deep learning; Arrow and arrowhead: equally well-segmented glomeruli despite the difference in aSMA stain; insert shows higher magnification of the segmentation of two glomeruli; D: Merging of signal in B and C with the glomerular surface in red and aSMA staining in green with co-localisation of the two signals represented as yellow pixels; Arrow: low aSMA expression within the glomerular area; Arrowhead: strong aSMA expression in the glomerular area; Insert: higher magnification of the glomerular structure. Immunoperoxidase (A) and digital image analysis (B, C, D); Scale bar = 350µm

Table 1: Example of different quantifications of aSMA expression in glomeruli in one of the kidneys.

aSMA expression quantifications	Result
Glomerular aSMA / Total glomerular area	0.37%
Glomerular aSMA/ Total kidney area	0.01%
Glomerular aSMA / Total kidney aSMA	2.39 %
Glomerular aSMA area	1463.24 micron2
Non-glomerular kidney aSMA area	59867.24 micron2

Discussion

The presented methodology showcases a successful quantification of alpha-smooth muscle actin (aSMA) expression within the glomeruli of a mouse kidney. The approach combines the traditional colour deconvolution technique with a deep learning algorithm, offering two distinct methods to extract information from immunohistochemically (IHC) stained sections. Deep learning algorithms can be trained on large datasets of histological images, allowing them to learn the complex patterns and relationships between different structures and cells. This can lead to accurate and reliable analysis of histological sections. This has been shown in several studies—however, most of those focus on the classification of traditional Haematoxylin-Eosin-stained sections (24). In our approach, we demonstrated that CNN could be efficiently trained to identify a microanatomical structure in an IHC (Haematoxylin and DAB) slide (in our case, the glomeruli) irrespective of the intensity of the IHC staining of such structures. This is clearly demonstrated in our results, as two glomerular structures that dramatically differ in the amount of aSMA positivity (almost absent vs. strong and diffuse) resulted in the correct identification of the glomerular class in the mask. This is due to the particular way of functioning of the CNNs, which gives relevance to patterns irrespective of stain intensities if the stains are not highly characteristic of the examples given during the training (25). The deep learning software employed in this study is based on Tensor Flow, an accessible AI open environment, alongside other software components utilised in constructing the workflow. The presented technique promises broad applicability through CNN's versatility and well-known applicability of colour deconvolution to DAB stain and potentially different chromogens and enzyme substrates, irrespective of the marker used, enabling the quantification of diverse protein biomarkers within different tissue compartments after training the CNN on samples from various micro-anatomical structures. In conclusion, the proposed methodology combines traditional colour deconvolution with deep learning techniques, providing a non-subjective and automated workflow for the quantification of aSMA expression in glomeruli. Leveraging the power of

CNNs and accessible software frameworks, this approach holds promise for quantifying other protein biomarkers within different tissue compartments, offering a valuable tool for histological analysis.

References

1. Csonka T, Murnyák B, Szepesi R, Bencze J, Bognár L, Klekner Á, Hortobágyi T. Assessment of candidate immunohistochemical prognostic markers of meningioma recurrence. Folia Neuropathol. 2016;54:114–126. doi: 10.5114/fn.2016.60088.

2. Hortobágyi T, Bencze J, Varkoly G, Kouhsari MC, Klekner Á. Meningioma recurrence. Open Med (Wars). 2016;11:168–173. doi: 10.1515/med-2016-0032. Cited: in: : PMID: 28352788.

3. Bencze J, Szarka M, Bencs V, Szabó RN, Módis LV, Aarsland D, Hortobágyi T. Lemur Tyrosine Kinase 2 (LMTK2) Level Inversely Correlates with Phospho-Tau in Neuropathological Stages of Alzheimer's Disease. Brain Sci. 2020;10:68. doi: 10.3390/brainsci10020068. Cited: in: : PMID: 32012723.

4. Updated: Semi-quantitative Determination of Protein Expression Using Immunohistochemistry Staining and Analysis. BIO-PROTOCOL [Internet]. 2023 [cited 2023 May 24];13. doi: 10.21769/BioProtoc.4610.

5. Johnson RJ, Iida H, Alpers CE, Majesky MW, Schwartz SM, Pritzi P, Gordon K, Gown AM. Expression of smooth muscle cell phenotype by rat mesangial cells in immune complex nephritis. Alpha-smooth muscle actin is a marker of mesangial cell proliferation. J Clin Invest. 1991;87:847–858. doi: 10.1172/JCI115089. Cited: in: : PMID: 1671868.

6. Kovacs GG, Xie SX, Lee EB, Robinson JL, Caswell C, Irwin DJ, Toledo JB, Johnson VE, Smith DH, Alafuzoff I, et al. Multisite Assessment of Aging-Related Tau Astrogliopathy (ARTAG). Journal of Neuropathology & Experimental Neurology. 2017;76:605–619. doi: 10.1093/jnen/nlx041.

7. Hanna W, O'Malley FP, Barnes P, Berendt R, Gaboury L, Magliocco A, Pettigrew N, Robertson S, Sengupta S, Têtu B, et al. Updated recommendations from the Canadian National Consensus Meeting on HER2/neu testing in breast cancer. Curr Oncol. 2007;14:149–153. Cited: in: : PMID: 17710207.

8. Walker RA. Quantification of immunohistochemistry—issues concerning methods, utility and semiquantitative assessment I. Histopathology. 2006;49:406–410. doi: 10.1111/j.1365-2559.2006.02514.x.

9. Deo RC. Machine Learning in Medicine. Circulation. 2015;132:1920–1930. doi: 10.1161/CIRCULATIONAHA.115.001593.

10. Bankhead P, Loughrey MB, Fernández JA, Dombrowski Y, McArt DG, Dunne PD, McQuaid S, Gray RT, Murray LJ, Coleman HG, et al. QuPath: Open source software for digital pathology image analysis. Sci Rep. 2017;7:16878. doi: 10.1038/s41598-017-17204-5.

11. Basheer S, Mañas A, Yao Q, Reiner K, Xiang J. Detection of melanin-mediated false-positive for BaxΔ2 immunohistochemical staining in human skin tissues [Internet]. Cell Biology; 2020 [cited 2023 May 31]. Available from: http://biorxiv.org/lookup/doi/10.1101/2020.10.30.361956.

12. Tsutsumi Y. Pitfalls and Caveats in Applying Chromogenic Immunostaining to Histopathological Diagnosis. Cells. 2021;10:1501. doi: 10.3390/cells10061501. Cited: in: : PMID: 34203756.

13. Silva FG, D'Agati VD, Nadasdy T. Renal biopsy interpretation. 1997;

14. Novakovic ZS, Durdov MG, Puljak L, Saraga M, Ljutic D, Filipovic T, Pastar Z, Bendic A, Vukojevic K. The interstitial expression of alpha-smooth muscle actin in glomerulonephritis is associated with renal function. Med Sci Monit. 2012;18:CR235–CR240. doi: 10.12659/MSM.882623. Cited: in: : PMID: 22460095.

15. Taye MM. Theoretical Understanding of Convolutional Neural Network: Concepts, Architectures, Applications, Future Directions. Computation. 2023;11:52. doi: 10.3390/computation11030052.

16. Srinidhi CL, Ciga O, Martel AL. Deep neural network models for computational histopathology: A survey. Medical Image Analysis. 2021;67:101813. doi: 10.1016/j.media.2020.101813.

17. Taylor A, Sharkey J, Harwood R, Scarfe L, Barrow M, Rosseinsky MJ, Adams DJ, Wilm B, Murray P. Multimodal Imaging Techniques Show Differences in Homing Capacity Between Mesenchymal Stromal Cells and Macrophages in Mouse Renal Injury Models. Mol Imaging Biol. 2020;22:904–913. doi: 10.1007/s11307-019-01458-8.

18. Ruifrok AC, Johnston DA. Quantification of histochemical staining by color deconvolution. Anal Quant Cytol Histol. 2001;23:291–299. Cited: in: : PMID: 11531144.

19. Helps SC, Thornton E, Kleinig TJ, Manavis J, Vink R. Automatic Nonsubjective Estimation of Antigen Content Visualized by Immunohistochemistry Using Color Deconvolution. Applied Immunohistochemistry & Molecular Morphology. 2012;20:82. doi: 10.1097/PAI.0b013e31821fc8cd.

20. Ronneberger O, Fischer P, Brox T. U-Net: Convolutional Networks for Biomedical Image Segmentation [Internet]. arXiv; 2015 [cited 2022 Aug 16]. Available from: http://arxiv.org/abs/1505.04597.

21. Markoulidakis I, Rallis I, Georgoulas I, Kopsiaftis G, Doulamis A, Doulamis N. Multiclass Confusion Matrix Reduction Method and Its Application on Net Promoter Score Classification Problem. Technologies. 2021;9:81. doi: 10.3390/technologies9040081.

22. Luchian A, Cepeda KT, Harwood R, Murray P, Wilm B, Kenny S, Pregel P, Ressel L. Quantifying acute kidney injury in an Ischaemia-Reperfusion Injury mouse model using Deep Learning-based semantic segmentation in histology. Biology Open. 2023;bio.059988. doi: 10.1242/bio.059988.

23. Schindelin J, Arganda-Carreras I, Frise E, Kaynig V, Longair M, Pietzsch T, Preibisch S, Rueden C, Saalfeld S, Schmid B, et al. Fiji: an open-source platform for biological-image analysis. Nat Methods. 2012;9:676–682. doi: 10.1038/nmeth.2019.

24. Zhao Y, Zhang J, Hu D, Qu H, Tian Y, Cui X. Application of Deep Learning in Histopathology Images of Breast Cancer: A Review. Micromachines (Basel). 2022;13:2197. doi: 10.3390/mi13122197. Cited: in: : PMID: 36557496.

25. O'Mahony N, Campbell S, Carvalho A, Harapanahalli S, Hernandez GV, Krpalkova L, Riordan D, Walsh J. Deep Learning vs. Traditional Computer Vision. In: Arai K, Kapoor S, editors. Advances in Computer Vision [Internet]. Cham: Springer International Publishing; 2020 [cited 2023 May 30]. p. 128–144. Available from: http://link.springer.com/10.1007/978-3-030-17795-9_10.

Acknowledgements:

Alder Hey Children's Kidney Fund supported this work. The authors thank NVIDIA for GPU support, Derek Magee for software assistance, the University of Liverpool – Leahurst histology laboratory for technical support and Silcock Veterinary Pathology Endowment for supporting slide scanner equipment in the DiMo lab. We thank Prof. Patricia Murray, Dr Bettina Wilm and Dr Rachel Harwood for providing the kidneys from previous ischaemia-reperfusion injury mouse surgeries.